Bispectrum of ship-radiated noise

Melvin J. Hinich
Applied Research Laboratories, The University of Texas at Austin, Austin, Texas 78713

Davide Marandino
ELSAG S.p.A., Via G. Puccini, 2, 16154 Genova-Sestri, Italy

Edmund J. Sullivan[a)]
SACLANT Undersea Research Centre, Viale San Bartolomeo 400, 19026 La Spezia, Italy

(Received 28 June 1988; accepted for publication 28 November 1988)

The bispectrum of ship-radiated noise is estimated. The noise was received on a towed array being towed by the same ship that served as the noise source. The array was beamformed such that the forward endfire beam pointed toward the towing platform and the broadside beam sampled the environment without the radiated noise of the ship. The results show that there exist frequency-dependent bispectral components in the ship's radiated noise, whereas the ambient noise does not contain any significant bispectral components. Since the existence of a nonzero frequency-dependent bispectrum indicates the existence of nonlinear components in the noise-generating mechanism, it is concluded that the radiated noise of the towing platform contains such nonlinear mechanisms. Therefore, the bispectrum could be used to indicate the existence of such noise sources as would normally be hidden in the background noise when the usual spectral estimation procedures are applied.

PACS numbers: 43.30.Nb, 43.50.Lj, 43.60.Cg

INTRODUCTION

Recent work that uses bispectral analysis to characterize ocean acoustic noise gives strong evidence that shipping-dominated noise contains strong nonlinear components in its generating mechanisms where the ambient sources do not.[1] The value of the bispectrum is that it is able to distinguish via the Hinich test[2] whether or not the source of the data contains such nonlinear components. Standard statistical tests, which are based on second moments, are unable to make such a distinction.

Since these results suggest a means for differentiating between shipping noise and at least some of the other forms of ambient noise sources, it is of interest to make a positive identification of a specific ship as a source of the noise. Such an identification is made in this work, where we analyze data taken from a towed array where its towing platform served as the noise source. The array was beamformed in such a manner that it was possible to "switch" the source on and off. That is, bispectra were made of the records obtained with the main beam steered to forward endfire (toward the towing platform) and compared to bispectra of the records obtained when the main beam was at broadside. The bispectrum of the forward endfire data indicated a significantly larger content of nonlinearity than that of the broadside data.

I. NONLINEAR MECHANISMS AND MODELS

A stationary time series is defined to be *linear* if it can be modeled in the form

$$x(t) = \sum_m h(m)\epsilon(t-m), \tag{1}$$

where $\{\epsilon(n)\}$ is a "*pure*" noise process, i.e., the $\epsilon(t)$ variates are mutually *independent*. Thus white, i.e., uncorrelated Gaussian noise is pure noise as a consequence of the fact that its zero correlation implies independence if the joint density of the $\epsilon(t)$ is Gaussian. If the process is not Gaussian, then whiteness is not a sufficient condition for it to be pure noise. A generalization of Eq. (1), which forms a class of nonlinear models, is the Volterra expansion,[3] which is given by

$$\begin{aligned} x(t) = &\sum_m h(m)\epsilon(t-m) \\ &+ \sum_m \sum_n h(m,n)\epsilon(t-m)\epsilon(t-n) \\ &+ \sum_m \sum_n \sum_p h(m,n,p)\epsilon(t-m) \\ &\times \epsilon(t-n)\epsilon(t-p) + \cdots, \end{aligned} \tag{2}$$

where the $h(m,n,\ldots)$ are called the Volterra kernels. The higher-order terms in Eq. (1) represent the nonlinearities that would not be explicitly manifested by standard tests. An explicit example of this is the simple quadratic model considered by Priestley[4]:

$$x(t) = \epsilon(t) + \alpha\epsilon(t-2)\epsilon(t-1), \tag{3}$$

where $\{\epsilon(t)\}$ is pure noise. It is easy to show that $\{x(t)\}$ is white. Therefore, any whiteness test on $\{x(t)\}$ would confirm that it is white, and the erroneous conclusion would be drawn that there is no remaining model structure to fit.

From a more heuristic point of view, since the major effect of the nonlinearities is to cause intermodulation between the frequency components of the driving process, without phase information in addition to the spectral power, the presence of the nonlinearities will not be detected.

It can be seen from Eq. (2) that, even for relatively simple cases, nonlinear models can have a large number of pa-

[a)] Presently at the Naval Underwater Systems Center, Code 01V, Newport, RI 02841.

 0001-4966/89/041512-06$00.80

rameters. For this reason, most studies treat special cases as nonlinear AR, MA, or ARMA models. The bispectra of a representative set of these models were computed by Ashley *et al.*[5]

Ship-radiated noise would be expected to arise from two sources: hydrodynamic and mechanical. The major hydrodynamic source of ship-radiated noise is propeller cavitation, which can be expected to fall in the lower end of the spectrum, i.e., near the blade rate, but is quite broadband and falls off roughly as the square of the frequency.[6] Cavitation noise by its very nature is a nonlinear phenomenon since it arises from the formation of bubbles that can grow in a very nonlinear way. Direct radiation from other hydrodynamic sources, such as flow noise, would not be expected to make a strong contribution to the energy in the sonar frequency range. However, flow will play a major role by coupling energy into the ship's hull, which then can radiate acoustic energy into the water. Even in the case of small amplitude vibration of hull plates, any structural characteristics that produce a nonlinear Hooke's law phenomenon would constitute a nonlinear mechanism. From this point of view, it would be expected that along with cavitation, the nonlinear characteristics of the mechanical sources of noise such as hull plates and rotating machinery would also play a role in the bispectrum of ship-radiated noise.

Generally speaking, there do not seem to be many explicit examples in the literature connecting such physical processes to nonlinear time series. In an attempt to provide some motivation for the analysis contained in this work, it is pointed out that some of the models in Ref. 5 can be identified with mechanical systems. In particular, the example referred to as the "threshold AR" in Ref. 5 is given by

$$\begin{aligned} &x(t) = \beta x(t-1) + \epsilon(t), \\ &\beta = -0.5, \quad \text{if } x(t-1) < 1, \\ &\beta = 0.4, \quad \text{otherwise}, \end{aligned} \tag{4}$$

can be identified with an approximation to an overdamped harmonic oscillator with a threshold value for its damping coefficient. An example that identifies nonzero bispectra with mechanical sources is given by Sato *et al.*,[7] where gear noise is analyzed. Although they do not give a specific example of a time series associated with their physical model, the efficacy of bispectral analysis in identifying such mechanical sources of acoustic noise is demonstrated.

II. THE BISPECTRUM AS A TEST FOR NONLINEARITY AND NONGAUSSIANITY

The bispectrum of a time series $\{x(t)\}$ is defined to be the double Fourier transform of the third-order cumulant. That is,

$$B(\omega_1,\omega_2) = \sum_m \sum_n C_{xxx}(m,n) e^{-i(\omega_1 m + \omega_2 n)}, \tag{5}$$

where

$$C_{xxx} = E[x(t+m)x(t+n)x(t)]. \tag{6}$$

If $x(t)$ can be represented by Eq. (1), it follows that its power spectrum is given by

$$S(\omega) = \sigma^2 |G(\omega)|^2, \tag{7}$$

with

$$G(\omega) = \sum_m h(m) e^{-i\omega m}, \tag{8}$$

and

$$\sigma^2 = E[\epsilon^2]. \tag{9}$$

Thus if $\{x(t)\}$ is linear, the bispectrum can be expressed in the form

$$B(\omega_1,\omega_2) = \mu_3 G(\omega_1) G(\omega_2) G^*(\omega_1 + \omega_2). \tag{10}$$

Here, μ_3 is the third moment of ϵ, i.e.,

$$\mu_3 = E[\epsilon^3]. \tag{11}$$

The bispectrum has a principal domain that is triangular. This follows from its symmetries. Letting f_j and f_k label the two frequencies, the principal domain is defined by the inequalities $0 \leqslant j \leqslant N/2$; $0 \leqslant k \leqslant j$; $2j + k \leqslant N$, with N being the size of the data set. This principal domain is shown in Fig. 1, where it can be seen that it is divided into two regions that are labeled inner triangle (IT) and outer triangle (OT).

Hinich and Wolinsky show that if the sample rate of the data is equal to or exceeds the Nyquist rate, then the bispectrum in the OT is expected to be zero.[8] The appearance of nonzero values of the bispectrum in the OT is an indication of transient nonstationarity if the sampled data are not aliased.

The Hinich test is based on a prewhitened bispectral gain called the skewness function given by

$$\Gamma(\omega_1,\omega_2) = \frac{|B(\omega_1,\omega_2)|}{[S(\omega_1)S(\omega_2)S(\omega_1+\omega_2)]^{1/2}}. \tag{12}$$

From Eqs. (7) and (10), we see that if $\{x(t)\}$ is linear, it immediately follows that

$$\Gamma^2(\omega_1,\omega_2) = \mu_3^2/\sigma^6. \tag{13}$$

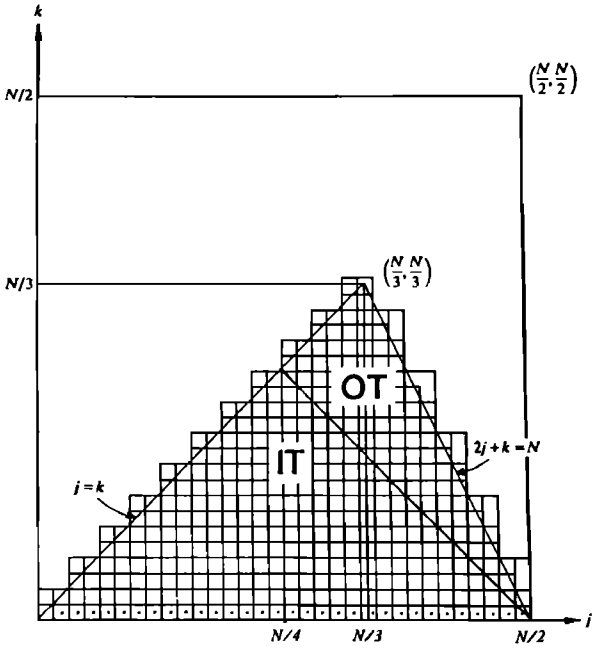

FIG. 1. Frequency plane lattice in the principal domain. N is the block length.

For a linear process then, the skewness is constant over the frequency plane. Note that since $\mu_3 = 0$ for the Gaussian case, a nonzero value of the bispectrum rejects Gaussianity. Consequently, all nonlinear processes are non-Gaussian.

In order to test for non-Gaussianity, Hinich compares a normalized estimate of $\Gamma^2(\omega_1,\omega_2)$ at different points on the ω plane to a central chi-squared distribution with two degrees of freedom (df). The chi-squared statistics are summed over a grid of bifrequencies (frequency pairs) in the principal domain. Any significant deviation of the sum of these statistics from a chi square of $2P$ df is taken to be a rejection of the Gaussian assumption. Here, P is the number of bifrequencies in the principal domain.

If the process is linear but not Gaussian, then the scaled estimate of $\Gamma^2(\omega_1,\omega_2)$ has a noncentral chi-squared distribution with two df and a noncentrality parameter that is the scale times $\Gamma^2(\omega_1,\omega_2)$.

The test used by Hinich for linearity is based on the dispersion of the estimate of the chi-squared statistics, assuming a constant noncentrality parameter that is estimated from the data. The noncentrality parameter for each chi-squared statistic is the squared skewness function at that bifrequency scaled by the normalization constant. Thus if the process is linear, the skewness is constant, implying that all the noncentrality parameters are equal. This dispersion is computed for a given fractile range and compared to the dispersion over the same fractile range for a Gaussian process. If this dispersion significantly exceeds that of the linear process, the assumption of linearity is rejected.

Hinich originally used the inner quartile range for this test.[2] However, here we shall use the 80th percentile range since it seems to be quite robust. For more details of these tests the FORTRAN code along with an instruction file may be obtained upon request. Also, see the appendix in Ref. 1.

III. DATA CHARACTERISTICS

As mentioned in the Introduction, the data were taken from a towed array. The towing platform was the MARIA PAOLINA G., the former research vessel of the SACLANT Undersea Research Centre. It has a length of 70 m, a beam of 12 m, and a draft of 4.5 m. Its displacement is 2800 metric tons. The engine is a six-cylinder, two-stroke, single-action diesel with 1800 BHP. At a speed of 5 kn, the shaft speed is 110–115 turns per min. The fixed-pitch propeller has five blades.

The array was towed at a speed of 5 kn at a depth of 70 m with a scope of 750 m. This placed it at the top of the thermocline. There was a weak sound channel at 100 m. The area used was the Ionian basin region of the Mediterranean Sea where the depth is about 2500 m. The weather was good with a sea state of 2. There was no shipping in the immediate area.

The data consist of two records, each taken at different times during the same day, which will be referred to as file 1 and file 2. Each record contains 50 s of endfire data and 50 s of broadside data. The spectrum had a flat region about 120 Hz wide with a center frequency of 1090 Hz. These spectrum characteristics are a consequence of the fact that the data were filtered with a linear phase Parks–McClellan filter with 127 coefficients and an out-of-band attenuation of 54 dB. The spectra for the broadside and endfire cases for file 1 are shown in Fig. 2. The towed array was made up of 40 elements with an interelement spacing of 49 cm. Thus the data are spatially oversampled.

The two data records consist of slightly more than 30 800 observations. These records were divided into blocks and then averaged over these blocks. Two block lengths were used in the actual calculation. These had lengths of 140 and 160. Since the sample interval was 0.0016 s, the respective bandwidths were 4.46 and 3.85 Hz. The number of observations allowed an average over 220 blocks for the block length of 140 and an average over 192 blocks for the block of length 160. The spectra and bispectra were then computed using these averaged blocks.

IV. RESULTS

As was pointed out in Sec. II, the bispectrum has a triangular principal domain. This is divided into an IT and an OT where the bispectrum is zero in the outer triangle for the case of Nyquist sampling. The bispectrum in this domain is thus expected to be nonzero in the case of transients. In Table I, the statistic that tests for Gaussianity is tabulated, both for the complete principal domain and the OT only. This statistic is based on the chi-squared distribution function for the case of $2P$ df, where P is the number of frequency pairs in the domain under test. Thus under the null hypothesis of Gaussianity, the statistic would be expected to be a sample from such a distribution. The statistic is presented in units of the standard deviation under the Gaussian assumption. It can be seen from Table I that in all cases the endfire data in the principal domain, are strongly non-Gaussian. For the case of the broadside data in the principal domain, only the data from file 1 are strongly non-Gaussian. This could be due to leakage of ship-radiated noise into the sidelobes of the array pattern. In the OT, the endfire data from both data files are

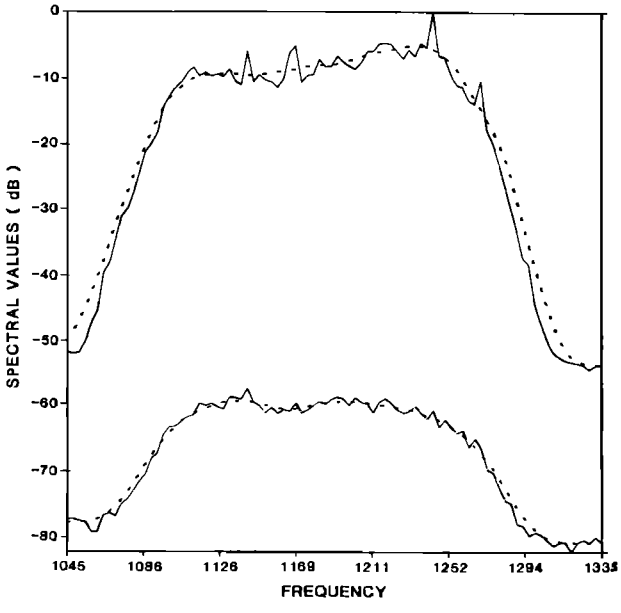

FIG. 2. Spectrum of the data record designated as file 1. Upper and lower curves correspond to the endfire and broadside cases, respectively. The dashed line indicates the smoothed spectrum.

TABLE I. Gaussianity statistics for the two block lengths of 140 and 160. B1 and E1 correspond, respectively, to the broadside and endfire cases for file 1. Similarly, B2 and E2 correspond to broadside and endfire for file 2.

Data set	Principal domain	Outer triangle
	Block size = 160	
B1	3.09	0.28
E1	13.15	7.86
B2	1.89	0.06
E2	30.77	13.50
	Block size = 140	
B1	4.02	1.68
E1	13.29	5.36
B2	0.36	− 1.79
E2	24.84	11.84

strongly non-Gaussian, and the broadside data from both files are not. The conclusions hold for both block sizes.

The statistic that tests for nonlinearity is the amount by which the 80th percentile exceeds the same percentile under the null hypothesis that the skewness is constant, which is *implied* by a *linear* hypothesis. It is in units of the standard deviation under the Gaussian assumption. This statistic is tabulated in Table II. As in the case of the Gaussian statistic, we present the results for the principal domain and also for the OT only. Here it can be seen that the endfire data from both files and for both block sizes are strongly nonlinear. In the case of the broadside data, the statistic indicates a small but statistically significant nonlinear component, especially in the case of the data from file 1. As in the case of the Gaussianity test, this is most likely due to leakage of ship-radiated noise into the sidelobes of the array beam pattern. As can be seen from Fig. 2, the endfire data are slightly more than 50 dB above the broadside data in level. Therefore, since the sidelobe rejection ratio could not be expected to be anywhere near this amount, it is not surprising to find such leakage. It would be difficult to estimate the actual rejection ratio of the array in this situation since the true angle of the radiation from the towing platform with respect to the array was not known.

In order to give some feeling for the bispectral levels

TABLE II. Linearity statistics for the two block lengths of 140 and 160. B1 and E1 correspond, respectively, to the broadside and endfire cases for file 1. Similarly, B2 and E2 correspond to broadside and endfire for file 2.

Data set	Principal domain	Outer triangle
	Block size = 160	
B1	2.32	0.63
E1	9.68	5.54
B2	1.25	− 0.21
E2	14.93	6.21
	Block size = 140	
B1	2.13	1.53
E1	7.63	3.35
B2	− 0.22	− 1.84
E2	11.14	6.12

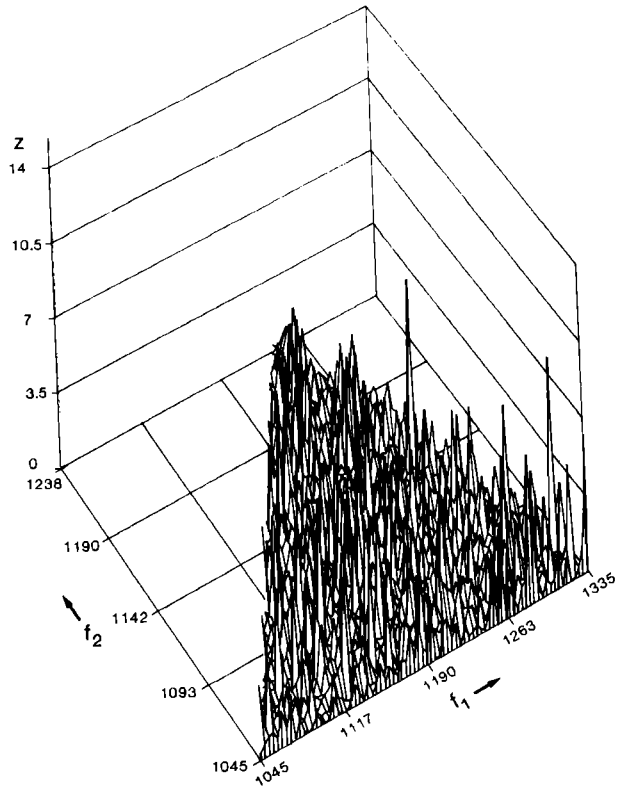

FIG. 3. Bispectrum values for the broadside case using the data record designated as file 1. The block size is 160.

associated with the statistics presented in Tables I and II, the bispectra for some selected cases along with their cumulative distribution levels above the 1% level under the Gaussian assumption are shown in Figs. 3–10. Only cases based on a

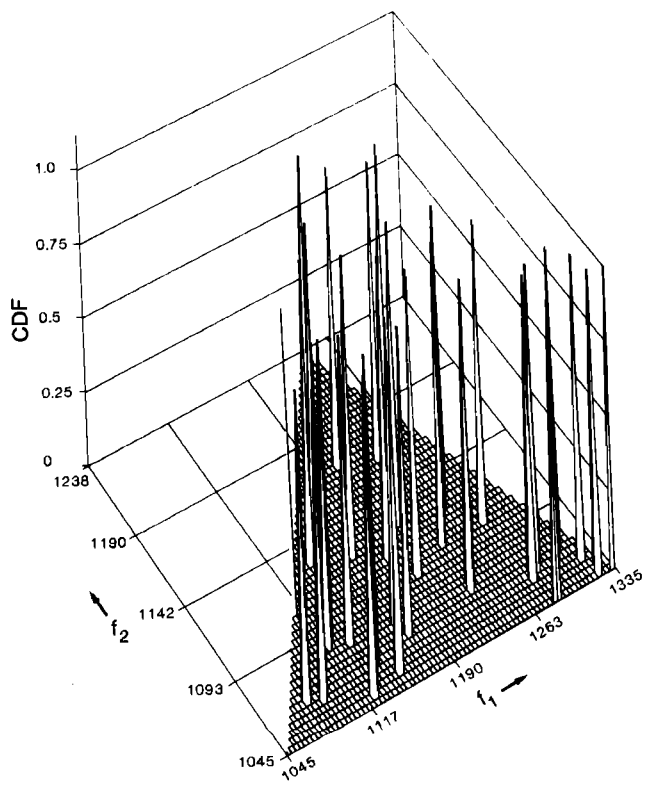

FIG. 4. Cumulative distribution values above the 1% level for the broadside case using the data record designated as file 1. The block size is 160.

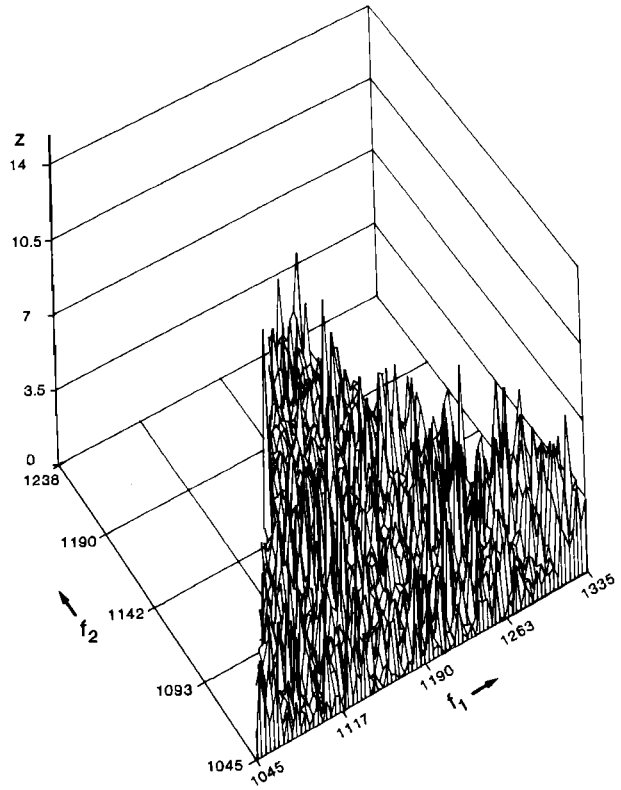

FIG. 5. Bispectrum values for the endfire case using the data record designated as file 1. The block size is 160.

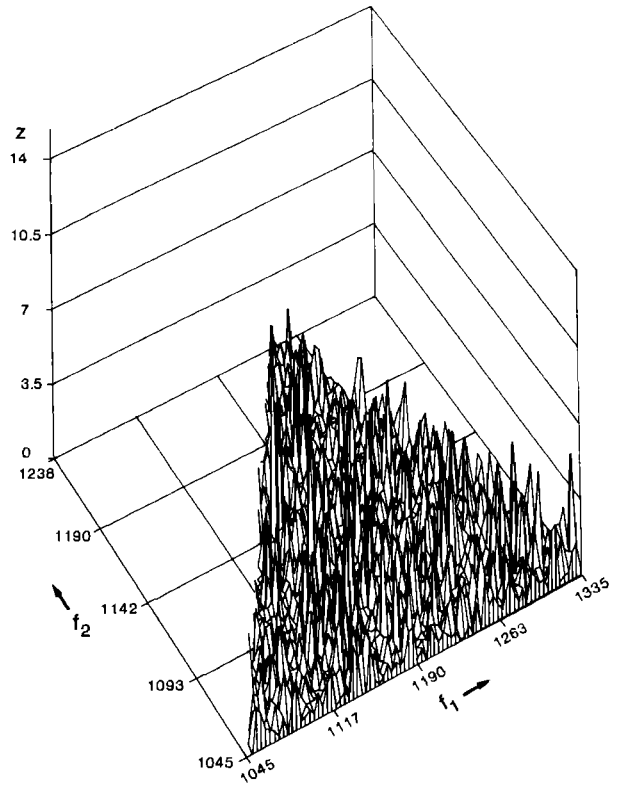

FIG. 7. Bispectrum values for the broadside case using the data record designated as file 2. The block size is 160.

block size of 160 are presented since there was no significant difference between these results and those for the block size of 140. The major differences occurred between the two data files, which would indicate some degree of nonstationarity in the data. Figures 3 and 4 depict the bispectrum and the associated cumulative distribution level for the case of the broadside data from file 1. In Fig. 4 and all similar figures that follow, only the cumulative distribution level above the 1%

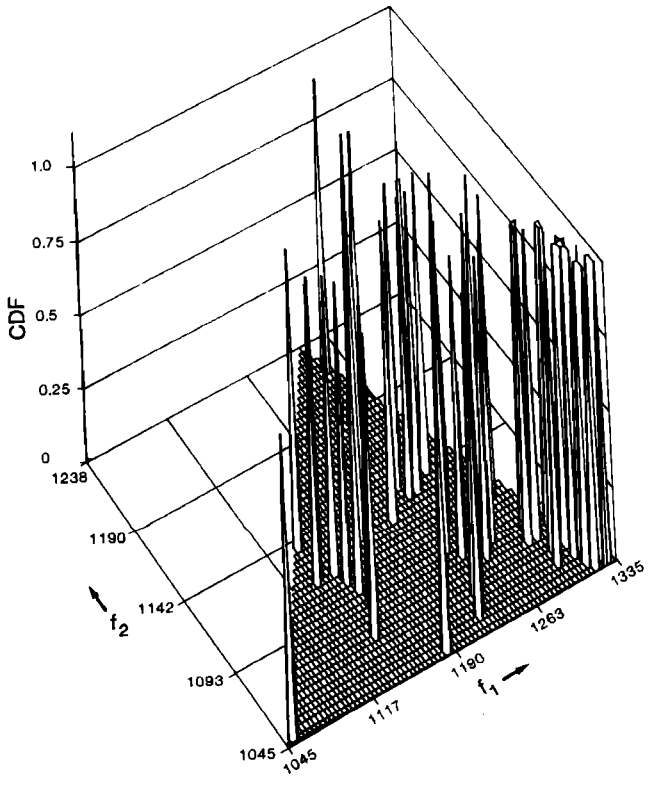

FIG. 6. Cumulative distribution values above the 1% level for the endfire case using the data record designated as file 1. The block size is 160.

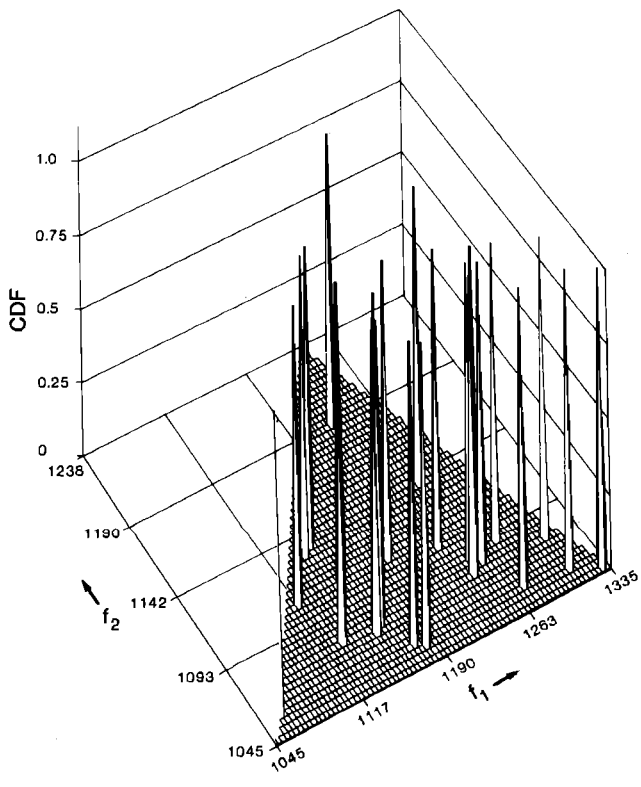

FIG. 8. Cumulative distribution values above the 1% level for the broadside case using the data record designated as file 2. The block size is 160.

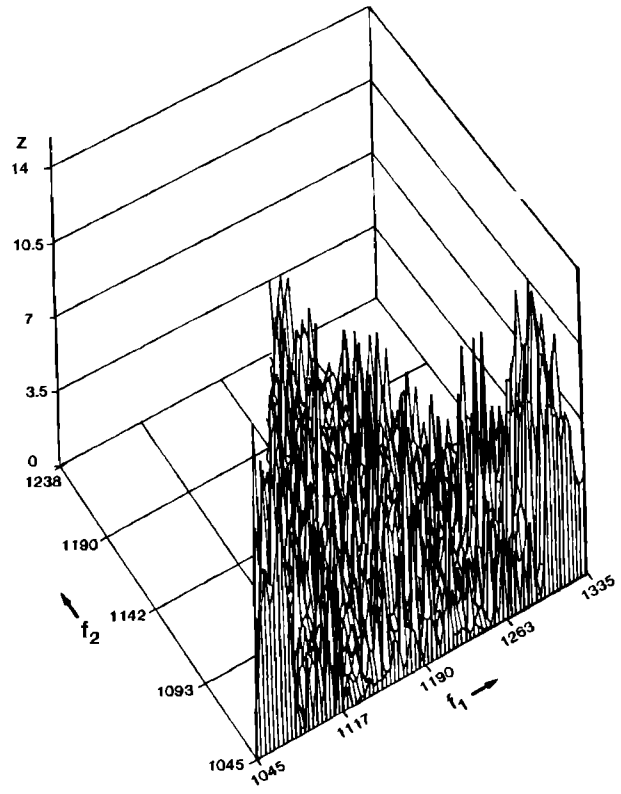

FIG. 9. Bispectrum values for the endfire case using the data record designated as file 2. The block size is 160.

levels are shown. Thus, these data levels have a probability of less than 1% under the Gaussian assumption. In Figs. 5 and 6, the endfire data corresponding to Figs. 3 and 4 are depicted. Figures 7 and 8 show the bispectrum and the associated cumulative distribution level under the Gaussian assumption for the case of the broadside data from file 2, and Figs. 9 and 10 show the endfire case corresponding to Figs. 7 and 8.

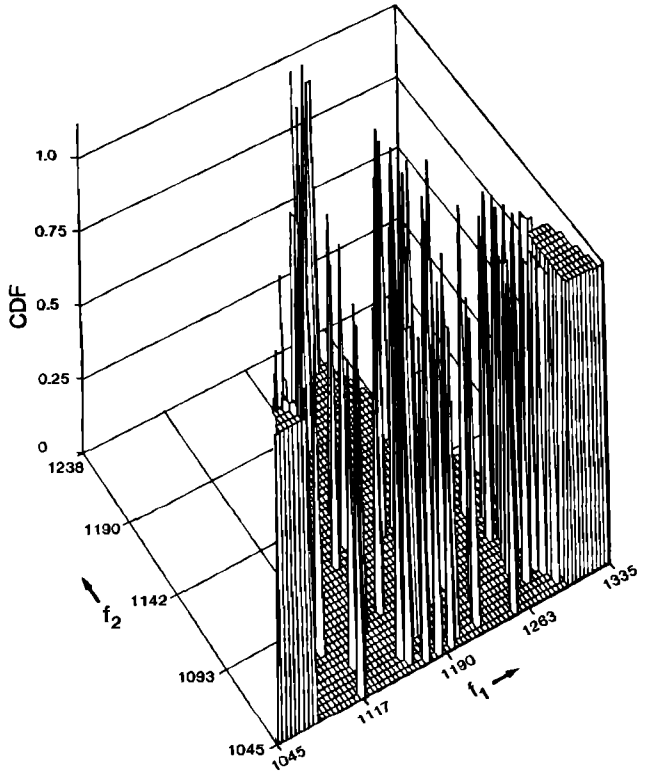

FIG. 10. Cumulative distribution values above the 1% level for the endfire case using the data record designated as file 2. The block size is 160.

V. CONCLUSIONS AND RECOMMENDATIONS

The major conclusion to be drawn from this study is that ship-radiated noise can be expected to contain a significant component of noise emanating from sources that contain nonlinear characteristics, and the bispectrum provides a means of detecting such sources. The results contained in this present study can be considered to be particularly significant since the data were quite narrow band, with a bandwidth of about 130 Hz and a center frequency of 1190 Hz—which corresponds to a bandwidth-frequency ratio of about 11%. Thus a great deal of the broadband-radiated noise was not considered by the bispectral calculation. In particular, the cavitation noise, which is expected to be the major contributor to the radiated noise, is out of band.

A second conclusion is that there appears to be a significant amount of transients in the data. If it were to be demonstrated that this is characteristic of ship-radiated noise in general, then this would serve as another indicator, along with the nonlinear character of the source, to identify ship-radiated noise in a strong background of ambient acoustic noise from other sources. Thus, the potential of bispectral analysis in obtaining an effective increase in processing gain in the detection of shipping noise in a strong ambient background is self-evident.

Another important point brought out by the results of this study is that in the application of the bispectrum to stochastic data, such as has been done here, it is important to rely on well-thought-out statistical indicators rather than direct observation of the bispectral plots themselves, as can be seen by comparing Figs. 3–10 to their corresponding statistics tabulated in Tables I and II. However, in this regard it should be added that the *configuration* of the bispectral plots themselves does contain information as to the particular type of nonlinearities associated with the data. Further studies in this direction would be of interest, particularly in regard to the problem of sonar classification. In this same vein, it would also be of interest to look at higher-order spectra, since there are certain classes of nonlinearities that do not manifest themselves in the bispectrum.[5]

[1]P. L. Brockett, M. J. Hinich, and G. R. Wilson, "Nonlinear and non-Gaussian noise," J. Acoust. Soc. Am. 82, 1386–1394 (1987).
[2]M. J. Hinich, "Testing for Gaussianity and linearity of a stationary time series," J. Time Series Anal. 3(3), 169–176 (1982).
[3]M. Schetzen, "Nonlinear system modeling based on the Wiener theory," Proc. IEEE 69 (112), 1557–1573 (1981).
[4]M. B. Priestley, *Spectral Analysis of Time Series* (Academic, London, 1981), Vol. II, p. 868.
[5]R. A. Ashley, D. M. Patterson, and M. J. Hinich, "A diagnostic test for nonlinear serial dependence in time series fitting errors," J. Time Series Anal. 7(3), 165–178 (1986).
[6]W. K. Blake, *Mechanics of Flow-Induced Sound and Vibration* (Harcourt Brace Jovanovitch, New York, 1986), Vol. II, Chap. 7.
[7]T. Sato, K. Sasaki, and T. Nakamura, "Real-time bispectral analysis of gear noise and its application to contactless diagnosis," J. Acoust. Soc. Am. 63, 1382–1387 (1977).
[8]M. J. Hinich and M. A. Wolinsky, "A test for aliasing using bispectral analysis," J. Am. Statist. Assoc. 83(402), 499–502 (1988).